EPJ manuscript No.
(will be inserted by the editor)

Spectral properties and stability in the Two-Dimensional Lattice-Hubbard model.

C. A. Lamas[1]

Departamento de Física, Universidad Nacional de La Plata, C.C. 67, 1900 La Plata, Argentina

Received: date / Revised version: date

Abstract. The two-dimensional Hubbard model on the square lattice is studied in the presence of lattice distortions in the adiabatic approximation. The self energy is computed within perturbation theory up to second order, which provides a way for studying the quasiparticle dispersion. We compute numerically the second order contribution to the self-energy using a standard Fast Fourier Transform Algorithm for finite sizes system. The stability of the lattice distortions is investigated and a schematic phase diagram is drawn. The Fermi surface is analyzed for densities close to half filling, the presence of lattice distortions changes some spectral properties of the model and gives an anisotropic interacting Fermi surface. The spectral function is calculated along several lines in momentum space and the renormalized quasiparticle dispersion is obtained. The behavior of the density of states is shown for different values of the intrasite repulsion U in the different phases.

PACS. 71.10.Fd Lattice fermion models – 63.20.kd Phonon-electron interaction

1 Introduction

The two dimensional Hubbard model has been usually associated with magnetism and superconductivity and is a promising toy model for the electronic degrees of freedom of high-temperature superconductors. The most interesting properties occur mostly in underdoped samples, with electron densities close to half filling, where the system is an antiferromagnetic Mott-insulator. The competition between the kinetic and Coulomb terms gives rise to strong electron-electron correlations.

The Peierls instability towards a spatially broken symmetry state in one dimensional systems is caused by the competition between the energy of lattice distortions and the formation of gap at the Fermi level in the electronic spectrum. This instability can occur in two dimensions if

the structure of the Fermi surface has a strong nesting by a single vector. It is the case of the two-dimensional square lattice in the tight-binding approximation at half filling.

Elastic Umklapp scattering with momentum transfer of (π, π)[1] across the Fermi Surface is allowed when it extends to the Brillouin zone boundary at half filling. In this case, a small electron-lattice coupling will induce a lattice dimerization which is related with a periodic modulation of the bond hopping called in the literature, bond-order wave (BOW). This motivates the study of the typical patterns for elastic deformations with modes corresponding to the nesting vector (π, π).

Although a finite frequency for the phonons would be important to study their influence in the mechanism of high Tc superconductivity, considering them as adiabatic could shed light on their influence on the different inhomogeneous phases that have been observed, e.g. in the underdoped region. Besides, their role is expected to be important for the undoped parent compounds.

Electron phonon coupling can lead to charge inhomogeneities, such as stripes, as has been studied in [2] within a spin-fermion model. However, this happens far from half-filling and for sufficiently strong diagonal coupling.

On the other hand, the lattice distortions change the Fermi Surface (FS) shape and the FS deformation due to the presence of interactions is a central question within the breakdown of the Fermi liquid theory. [3,4,5,6]

In the strong coupling regime one can find not only a deformed FS, but may even find a different topology. The FS of the non interacting Hubbard model is closed around the origin in the reciprocal space while in the interacting case it can be a surface closed around the point (π, π). It is in this regime where the role of the elastic distortions can take an important place in the high temperature superconductor phases [7]

In this paper we study the stability of lattice distortions in the presence of Coulomb interactions U. The critical values U_c where the distortions are suppressed are studied and a schematic phase diagram is drawn. The spectral properties are analized in the region of parameter space where the elastic deformations are favored and the FS shape is constructed from the renormalized dispersion. The FS shape was studied for the Hubbard model in the last years [8,9,10,11,12,13], but the influence of lattice distortions has not been taken into account. The Polaron formation in the Holstein-Hubbard model was investigated in [14] by means the slave-boson saddle-point approximation and the $t-J$ model with electron-phonon interaction was studied recently [15] for small systems. We show that these distortions have an influence in the FS shape leading to an anisotropic FS in the $\delta \neq 0$ phase.

2 Second order Perturbation theory.

2.1 The model

We examine the Hubbard model, coupled with a classical phonon field , which describes spin-$\frac{1}{2}$ fermions in a two dimensional square lattice with nearest-neighbor interactions, in the presence of lattice distortions in the adiabatic approximation. This model represent a useful toy model to

describe the physic in the presence of vibrational modes . The dependence of the hopping amplitudes $t_{i,j}$ is assumed to be linear in the lattice distortions.

$$
\begin{aligned}
H = & -t_0 \sum_{\sigma} \sum_{i=1}^{L} \sum_{j=1}^{L} (1+\alpha(u^x_{i+1,j} - u^x_{i,j}))\; c^{\dagger}_{i,j,\sigma} c_{i+1,j,\sigma} \\
& + (1+\alpha(u^y_{i,j+1} - u^y_{i,j})) c^{\dagger}_{i,j,\sigma} c_{i,j+1,\sigma} + \text{H.c}) \qquad (1) \\
& + U \sum_{i,j} n_{i,j\uparrow}\, n_{i,j\downarrow} \\
& + \frac{K}{2} \sum_{i,j} ((u^x_{i+1,j} - u^x_{i,j})^2 + (u^y_{i,j+1} - u^y_{i,j})^2),
\end{aligned}
$$

where t_0 is the transfer integral between nearest neighbor

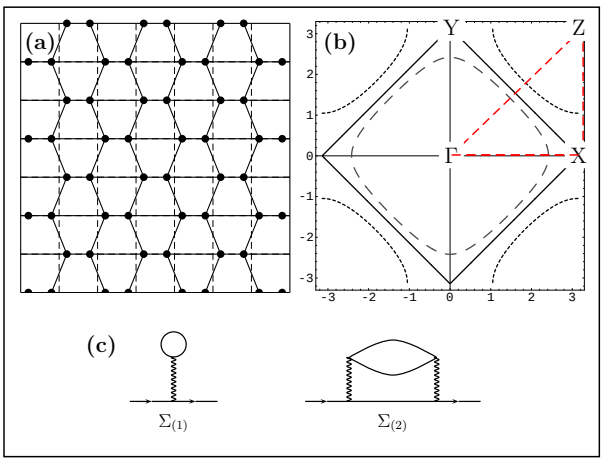

Fig. 1. a) Lattice shape for the modulations corresponding to pattern (a). **b)** Fermi surfaces for various densities ρ in the two-dimensional free fermion case. For densities $\rho < 1$ the FS is centered in the Γ-point and for $\rho > 1$ it is centered in the Z-point. **c)** Diagrams which contribute to the self energy up to second order in U. The wavy lines represent the on site repulsive interaction and the solid lines the free propagators.

sites in the absence of distortions, $n_{i,j,\sigma} = c^{\dagger}_{i,j,\sigma} c_{i,j,\sigma}$ is the number operator for electrons of spin σ at site i, α is the electron-phonon coupling, K is the elastic constant of the lattice and U is the on site Hubbard interaction. It is convenient to work with the dimensionless parameters

$$\delta^x_{i,j} = \alpha(u^x_{i+1,j} - u^x_{i,j}) \qquad (2)$$

$$\delta^y_{i,j} = \alpha(u^y_{i,j+1} - u^y_{i,j}) \qquad (3)$$

$$\lambda = \frac{\alpha^2 t_0}{K} \qquad (4)$$

and in the following we fix the energy scale setting $t_0 = 1$.

We first review briefly the free case ($U = 0$) and $\delta^{x,y} \equiv 0$, where:

$$\varepsilon_0(\mathbf{k}) = -2(\cos k_x + \cos k_y). \qquad (5)$$

The FS for different densities ρ is shown in Figure 1-b, for half-filling ($\rho = 1$) being a diamond centered at the origin with vertices at $\pm(0,\pi)$ and $\pm(\pi,0)$.

Let us consider the two possible alternation patterns consistent with the nesting vector $Q = (\pi,\pi)$:

$$
\begin{aligned}
\delta^x_{i,j} &= (-1)^{i+j}\delta^x_0 \qquad \text{or} \qquad \delta^x_{i,j} = (-1)^{i+j}\delta^x_0 \\
\delta^y_{i,j} &= 0 \qquad\qquad\qquad\quad \delta^y_{i,j} = (-1)^{i+j}\delta^y_0, \qquad (6)
\end{aligned}
$$

namely patterns (a) and (b) respectively [16]. The two dimensional Peierls instability in the pure-hopping case was studied by Tang and Hirsch [17] founding that at half filling pattern (a) is favored. Using a Mean Field (MF) approach we can see that for a wide range of values of U this pattern survives up to a critical value U_c. First we review the MF results and later, by using second order perturbation theory we reexamine the stability of the distortions in the present model.

When one considers a non trivial Hubbard local interaction, it is easy to see, using Hartree-Fock [18], that for

$U < U_c$ distortions (a) are favored at half filling and for $U > U_c$ the distortions are quickly suppressed.

Treating the local Coulomb repulsion in the MF approximation,

$$U\sum_{i,j} n_{i,j,\uparrow}n_{i,j,\downarrow} \rightarrow U\sum_{i,j}(\langle n_{i,j,\uparrow}\rangle n_{i,j,\downarrow} + \langle n_{i,j,\downarrow}\rangle n_{i,j,\uparrow} - \langle n_{i,j,\uparrow}\rangle\langle n_{i,j,\downarrow}\rangle) \quad (7)$$

the hamiltonian becomes quadratic and it is straightforwardly diagonalized in reciprocal space.

The expectation value $\langle n_{i,j}\rangle$ is assumed uniform, and the electron density with a given spin can be assumed as $\langle n_{i,j,\sigma}\rangle = \frac{1}{2} + \frac{\sigma}{2}(-1)^{i+j}m$ [18], m being the staggered magnetization. Within this approximations the electronic spectra for the two patterns (a) and (b) are

$$\varepsilon^{(a)}(\mathbf{k})_{\pm} = \pm 2t\sqrt{\frac{U^2m^2}{4} + 4(\cos k_x + \cos k_y)^2 + 4\delta^2\sin^2 k_x} \quad (8)$$

$$\varepsilon^{(b)}(\mathbf{k})_{\pm} = \pm 2t\sqrt{\frac{U^2m^2}{4} + 4(\cos k_x + \cos k_y)^2 + 4\delta^2(\sin k_x + \sin k_y)^2}$$

The ground state energies for the two patterns are

$$E = \frac{2}{L^2}\sum_k \varepsilon^{a(b)}(k)_- + \frac{U}{4}(1+m^2) + r\frac{\delta^2}{2\lambda} \quad (9)$$

with $r = 1$ for pattern (a) and $r = 2$ for pattern (b).

Minimizing the energy with respect to δ and m for various values of U and λ we can easily see that pattern (a) has lower energy than pattern (b) and for a huge range of U the values of δ^*_{MF} for minimum energy are almost constant.

For example for $\lambda = 0.5$ we have for pattern (a) $\delta^*_{MF} \simeq 0.24$ and for pattern (b) $\delta^*_{MF} \simeq 0.13$. The value of the interaction where the distortions are suppressed is $U_c \sim 2$.

In the presence of distortions that follow pattern (a) the lattice changes as we show in Figure 1-a. The unit cell is doubled and the Brillouin Zone is reduced to half. It is straightforward to find the electronic spectra for the deformed free case $(U = 0)$. Working in the first Brillouin zone (BZ) we have two single particle bands

$$\tilde{\varepsilon}_0(\mathbf{k})_{\pm} = \pm 2t\sqrt{(\cos k_x + \cos k_y)^2 + \delta^2\sin^2 k_x}.$$

for pattern (a) and

$$\tilde{\varepsilon}_0(\mathbf{k})_{\pm} = \pm 2t\sqrt{(\cos k_x + \cos k_y)^2 + \delta^2(\sin^2 k_x + \sin^2 k_y)}.$$

for pattern (b). In the following we will work in the extended Brillouin zone formed by a square centered in the point $\Gamma = (0,0)$ with vertices in $\pm Z$ and $\pm\bar{Z}$ where $Z = (\pi,\pi)$ and $\bar{Z} = (\pi,-\pi)$. The unperturbed dispersion in the extended BZ is

$$\varepsilon(\mathbf{k}) = 2(1 - 2\,\theta(\eta(\mathbf{k})))\sqrt{\eta(\mathbf{k})^2 + \delta^2\sin^2 k_x} \quad (10)$$

$$\varepsilon(\mathbf{k}) = 2(1 - 2\,\theta(\eta(\mathbf{k})))\sqrt{\eta(\mathbf{k})^2 + \delta^2(\sin^2 k_x + \sin^2 k_y)} \quad (11)$$

for patterns (a) and (b) respectively, where we have used $\eta(\mathbf{k}) = \cos k_x + \cos k_y$ and θ is the step function. In order

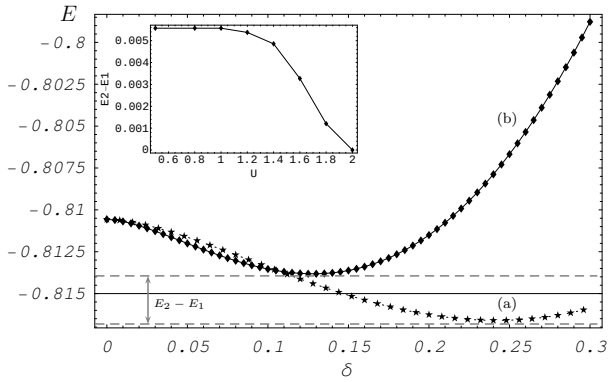

Fig. 2. Energy calculated for both patterns (a) stars and (b) squares as a function of δ for $U = 0.4$, $\lambda = 1/2$ and $m = 0$. Clearly pattern (a) has lower energy. On the other hand it is easy to see that the value of δ in the minimum energy is almost constant in the range of U between 0 and ~ 2. In the Inset the difference of energy between the two patterns is shown as a function of U, this difference falls off to zero at $U_c \approx 2$ where the distortion δ its suppressed.

to fix the notation we present here other important points used in this work like $X = (\pi, 0)$, $Y = (0, \pi)$ and $M = (\frac{\pi}{2}, \frac{\pi}{2})$.

2.2 Second order self energy

The contributions to the self energy are given by the diagrams shown in Figure. 1-c, these contributions were calculated using ordinary perturbation theory and were calculated slightly away half filling where divergences can appear. To deviate slightly half-filling are not significant changes in patterns of deformations in the mean field treatments and previous work showing that there is no appearance of stripes phase for fillings close to one [2].

Since the partners in the scattering processes have opposite spins, other possible diagrams with two Coulomb lines are absent.

The contributions of these diagrams are given by

$$\Sigma^{(1)}(\mathbf{k},\omega) = -U\frac{\imath}{(2\pi)^3}\int_{-\infty}^{\infty} d\omega' \int_{BZ} d^2\mathbf{k}' G^{(0)}(\mathbf{k}',\omega') = \frac{U\,\rho}{2}\,, \tag{12}$$

where ρ is the electronic density of the system and

$$\Sigma^{(2)}(\mathbf{k},\omega) = \frac{(U)^2}{(2\pi)^6}\int_{-\infty}^{\infty} d\omega' \int_{-\infty}^{\infty} d\omega'' \int_{BZ} d^2\mathbf{k}' \int_{BZ} d^2\mathbf{k}'' \times \times G^{(0)}(\mathbf{k}',\omega') G^{(0)}(\mathbf{k}'',\omega'') G^{(0)}(\mathbf{k}+\mathbf{k}'-\mathbf{k}'', \omega+\omega'-\omega'') \tag{13}$$

where

$$G^{(0)}(\mathbf{k},\omega) = \frac{1}{\omega - \xi_{\mathbf{k}} + \imath\gamma_{\mathbf{k}}} \tag{14}$$

with $\xi_{\mathbf{k}} = \varepsilon_0(\mathbf{k}) - \mu$, $\gamma_{\mathbf{k}} = \gamma\ \mathrm{sign}(\xi_{\mathbf{k}})$ and μ is the chemical potential.

To first order, the contribution of $\Sigma^{(1)}$ is a real constant ($\mathbf{k}$-independent) that shifts the dispersion relation and does not contribute to the FS deformation because it can be absorbed by a shift in the chemical potential $\delta\mu_1 = Un/2$ to keep the density fixed. The second order contribution to the self energy

$$\Sigma^2(\mathbf{k},\omega) = \frac{U^2}{L^2}\sum_{\mathbf{k'},\mathbf{k''}} \left(\frac{\theta(\xi_{\mathbf{k}-\mathbf{k'}})\theta(\xi_{\mathbf{k'}-\mathbf{k''}})\theta(-\xi_{\mathbf{k''}})}{\omega - \xi_{\mathbf{k}-\mathbf{k'}} - \xi_{\mathbf{k'}-\mathbf{k''}} + \xi_{\mathbf{k''}}} + \frac{\theta(-\xi_{\mathbf{k}-\mathbf{k'}})\theta(-\xi_{\mathbf{k'}-\mathbf{k''}})\theta(\xi_{\mathbf{k''}})}{\omega - \xi_{\mathbf{k}-\mathbf{k'}} - \xi_{\mathbf{k'}-\mathbf{k''}} + \xi_{\mathbf{k''}}} \right) \tag{15}$$

is $\mathbf{k}$-dependent producing a renormalized dispersion and leads to a FS deformation. This term is computed numerically in what follows using a Fast Fourier Transform (FFT) for finite size systems. The momenta in the Brillouin zone are discrete and defined by $k_{x,y} = -\pi + \Delta k(n_{x,y} - 1)$ and $\Delta k = \frac{2\pi}{L}$, $n_{x,y} = 1,\ 2,\ \ldots,\ L$

The retarded self energy in space-time representation is

$$\Sigma^{(2)}_{ret}(\mathbf{x},t) = \mathcal{F}_{\mathbf{k}}\mathcal{F}_{\omega}\left[\Sigma^{(2)}(\mathbf{k},\omega + i0^+)\right] = \frac{1}{L}\sum_{\mathbf{k}}\int_{-\infty}^{\infty}\frac{d\omega}{2\pi}\, e^{i(\mathbf{k}\cdot\mathbf{x}-\omega t)}\Sigma^{(2)}(\mathbf{k},\omega+i0^+) \tag{16}$$

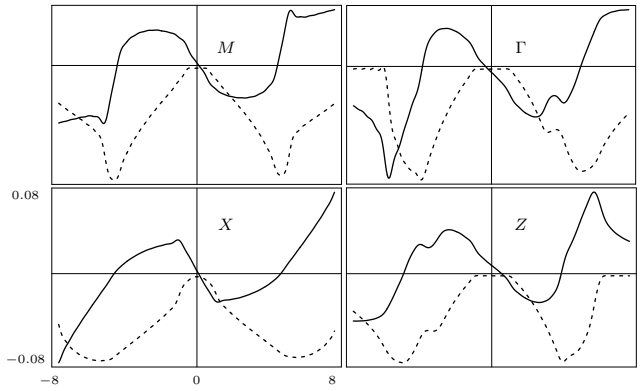

Fig. 3. Self Energy in M, Γ,X and Z points at $\rho = 0.995$, The solid line correspond to the real part and the dotted one to the imaginary part of the Self Energy.

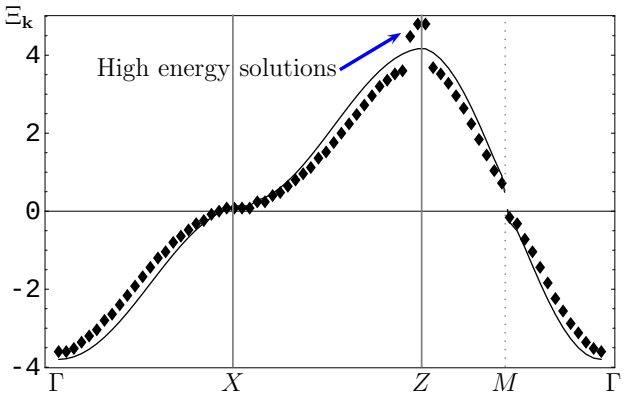

Fig. 4. Renormalized dispersion relation corresponding to $\delta = 0.24$ and $U = 1.8$ in the $\Gamma \to X \to Z \to \Gamma$ line. The squares correspond to the renormalized dispersion calculated by means of Eq. (21) and the solid line corresponds to the free case. We can see that the Coulomb interaction reduces the bandwidth. In the Z-point some high energy solutions appear.

where the Fourier transform is defined by

$$\mathcal{F}_{\mathbf{k}}\left[g(\mathbf{k})\right](\mathbf{x}) = \frac{1}{L}\sum_{\mathbf{k}} e^{i\mathbf{k}\cdot\mathbf{x}} g(\mathbf{k}) \tag{17}$$

$$\mathcal{F}_{\omega}\left[g(\omega)\right](t) = \int_{-\infty}^{\infty} \frac{d\omega}{2\pi} e^{-i\omega t} g(\omega) \tag{18}$$

and the inverse transformation is denoted by $\mathcal{F}_{\mathbf{k}}^{-1}$ and $\mathcal{F}_{\omega}^{-1}$ respectively

The frequency Fourier transform is straightforward

$$\Sigma^{(2)}_{ret}(\mathbf{x},t) = -\,i\,\theta(t)\frac{U^2}{L^2}\,\mathcal{F}_{\mathbf{k}}\left[\sum_{\mathbf{k'},\mathbf{k''}} z(\mathbf{k}-\mathbf{k'},t)z(\mathbf{k'}-\mathbf{k''},t)w^*(\mathbf{k''},t) + w(\mathbf{k}-\mathbf{k'},t)w(\mathbf{k'}-\mathbf{k''},t)z^*(\mathbf{k''},t)\right] \tag{19}$$

where we have used the short-hand notation

$$z(\mathbf{k},t) = e^{-i\xi_{\mathbf{k}}t}\theta(-\xi_{\mathbf{k}})$$

$$w(\mathbf{k},t) = e^{-i\xi_{\mathbf{k}}t}\theta(\xi_{\mathbf{k}}).$$

The transformation in $\mathbf{k}$ is the Fourier transform of a convolution and can be written as product of the Fourier transforms

$$\Sigma^{(2)}_{ret}(\mathbf{x},t) = -\,i\,\theta(t)\frac{U^2}{L^2}\,\left[\tilde{z}^2(\mathbf{x},t)\tilde{w}^*(\mathbf{x},t) + \tilde{w}^2(\mathbf{x},t)\tilde{z}^*(\mathbf{x},t)\right]$$

with $\tilde{z}(\mathbf{x},t) = \mathcal{F}_{\mathbf{k}}[z(\mathbf{k},t)]$ and $\tilde{w}(\mathbf{x},t) = \mathcal{F}_{\mathbf{k}}[w(\mathbf{k},t)]$

Clearly $\tilde{z}(\mathbf{x},t) = \langle c_{\mathbf{x}}(t)c^{\dagger}_{\mathbf{0}}(0)\rangle$ and $\tilde{w}(\mathbf{x},t) = \langle c^{\dagger}_{\mathbf{0}}(0)c_{\mathbf{x}}(t)\rangle$ and the causal free propagator in space-time is given by $G^0(\mathbf{x},t) = -i(\theta(t)\tilde{z}(\mathbf{x},t) - \theta(-t)\tilde{w}(\mathbf{x},t))$

The functions $\tilde{z}(\mathbf{x},t)$ and $\tilde{w}(\mathbf{x},t)$ can be calculated for finite size systems with a standard FFT algorithm. Then, replacing the result in the equation for $\Sigma^{(2)}_{ret}(\mathbf{x},t)$, we can obtain the self energy in momentum space by means of the inverse Fourier transform

$$\Sigma^{(2)}(\mathbf{k},\omega+i0^+) = \mathcal{F}^{-1}_{\mathbf{k}}\mathcal{F}^{-1}_{\omega}[\Sigma^{(2)}_{ret}(\mathbf{x},t)].$$

The real and imaginary parts of the self energy are shown in Figure 3 for M, Γ, X and Z points at $\rho = 0.995$. The shape of the Self Energy is very similar to the one found for the Hubbard model [19] but some features are δ-dependent. For example, in Figure 3 the real part of Σ in the point X has a clear linear behavior in a wide interval around $\omega = 0$. The range of ω where this occurs is larger for higher values of δ. The symmetries of the Hubbard model are preserved. We can see in Figure 3 that if one changes $\omega \to -\omega$ in the plot for the imaginary part of Σ at point Γ, the one corresponding to point Z is recovered. In the plots for the points Γ and Z it can be seen that $\Re\mathrm{e}\left\{\Sigma(\mathbf{k},\omega)\right\} = -\Re\mathrm{e}\left\{\Sigma(\mathbf{k}+\mathbf{Q},-\omega)\right\}$, with $\mathbf{Q} = (\pi,\pi)$.

The interacting Green function [20] can be calculated up to second order

$$G(\mathbf{k},\omega+i0^+) = \frac{1}{\omega+i0^+ - \xi_{\mathbf{k}} - \Sigma(\mathbf{k},\omega+i0^+)} \tag{20}$$

and the low energy excitations can be determined from the equation

$$G^{-1}(\Omega, \mathbf{k}) = \Omega - \xi_{\mathbf{k}} - \Re e \Sigma(\mathbf{k}, \Omega) = 0. \qquad (21)$$

For each point in the Brillouin zone, the last equation gives the renormalized dispersion as a function of the chemical potential

$$\Xi_{\mathbf{k}} = \Omega. \qquad (22)$$

In Figure 4 we show the renormalized dispersion for $U = 1.8$ in the path shown in Figure 1. We can see that the Coulomb interaction reduces the bandwidth.

For values of the momentum away from the FS, in particular for high values of U, Eq. (21) can give more solutions corresponding to higher energy excitations. This is particularly clear in the points Γ and Z where two new bands appear for $U > 1$. This is reminiscent of the Hubbard bands. Figure 4 shows the high energy solutions in the Z-point. We chose to show a result for a high value of U because the effects of renormalization are more evident and then the high energy solutions are visible.

2.3 Stability of lattice distortions.

The Ground State energy per site was calculated for several values of U and λ

$$E = \frac{2}{(2\pi)^2} \int d^2\mathbf{k}\ \Xi_{\mathbf{k}}(\delta)\theta(-\Xi_{\mathbf{k}}(\delta)) + r\frac{\delta^2}{2\lambda} \qquad (23)$$

where $r = 1$ for pattern (a) and $r = 2$ for pattern (b)

Keeping fixed the filling, we can calculate the energy for various values of δ and λ as a function of U. In this way we can study the stability of the lattice distortions when increasing the Coulomb interaction U, beyond the Mean Field approximation. In the following we restricted ourselves to study pattern (a) . The values of δ that minimize the total energy depend of λ and when $\lambda \to 0$, the distortions are suppressed. In our calculations the deformations are suppressed for values below some λ finite since the calculations were made for finite size systems (in general for systems of 120×120 sites, but the spectral properties are not severely changed for bigger sizes.) In Figure 5 we show the energy as a function of U for $\lambda = 0.5$ and several values of δ. We can see that for $U < U_c$ the curves have a minimum for a non trivial value of δ and that for

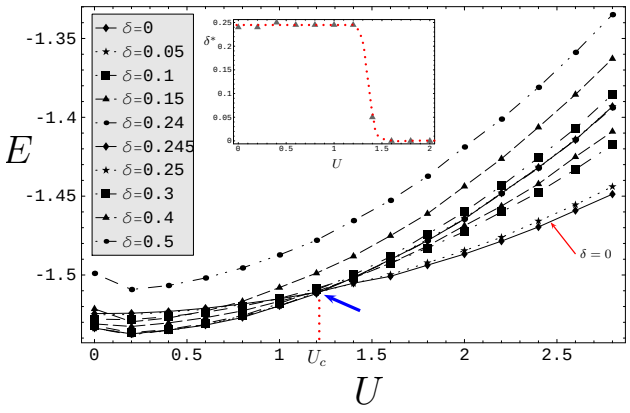

Fig. 5. Energy per site vs U for several values of δ corresponding to $\lambda = 0.5$ and $\rho = 0.995$. For $U_c \sim 1.21$ there is a crossing between the curves and for $U > U_c$ the minimum energy corresponds to $\delta = 0$. In the inset we show the optimal value δ^* that minimizes the energy as a function of U. For $U > U_c$ the distortions are suppressed and for $0 \leq U < U_c$ the parameter δ takes an optimal value δ^* for most of the values of U and there is one narrow region near U_c where δ goes quickly to zero.

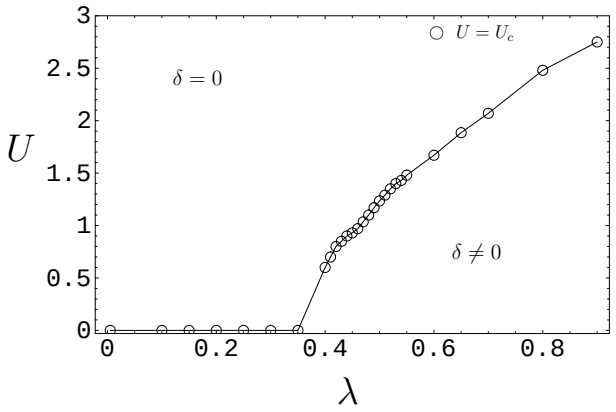

Fig. 6. Schematic phase diagram. The curve corresponds to $U = U_c$.

$U > U_c$ the minimum energy is reached for $\delta = 0$. The δ^*-value for minimum energy is plotted as a function of U in the Inset of Figure 5 where we can see clearly that δ^* stays almost constant for values of U smaller than U_c and it tends quickly to zero in a narrow region $U \sim U_c$. The critical value U_c that we found in our approach is lower than the one found in [18] by means of a MF approach, but the corresponding values of δ^* are very similar.

In Figure 6 we show schematically the regions in the (λ, U) space where δ takes non trivial values, this region is labelled as $\delta \neq 0$. The curve in Figure 6 shows the values found for U_c. For each value of λ we have $\delta = 0$ for the U-values above the critical curve. The two dimensional Hubbard model with $U > 0$ at half filling has AFM long range order, however, to depart slightly from this point we can not ensure that this order is maintained in the system without properly studying the AFM order parameter, but as the main subject of this work is the study of the stability of elastic deformations and their influence in the spectral properties, we labeled this phase simply as $\delta = 0$ or non-elastic phase. In the region below the critical curve, where the elastic deformations becomes stable, the phase is labeled by $\delta \neq 0$ or elastic phase. For points close and below the critical curve there is a small region where the δ-values rise from 0 to δ^*, as can be seen in the inset of Figure 5.

For fixed values of the Coulomb interaction the electron-lattice constant λ governs the phase of the system, and for this reason it could be interesting to compare the properties of the system at fixed U for $\delta = 0$ and $\delta = \delta^*$. In the following we show some of the spectral properties calculated for the model in the elastic phase.

2.4 Spectral properties in the presence of elastic distortions .

The single-particle spectral function $A_{\mathbf{k}}(\omega) = -\frac{1}{\pi}\Im m G(\mathbf{k}, \omega)$ is calculated in the second order approximation. In Figure 7 we show the spectral function along the lines $\Gamma \rightarrow Z$, $Y \rightarrow Z$, $X \rightarrow Z$ and $\Gamma \rightarrow X$ for $U = 1$ in the $\delta \neq 0$ phase. The behavior of the spectral function is seen to be different from the one found in the region with $\delta = 0$ [19]. The peaks in the spectral function for this case are broader and asymmetric for $\mathbf{k}$ far from the FS, while for the case with distortions the symmetry is preserved and the peaks are narrower. In the $\delta = 0$ case at higher energies the quasiparticle peaks decay very slowly while in the $\delta \neq 0$ case the peaks decay more quickly. The splitting in the spectral function seen for $\delta = 0$ is absent in the $\delta \neq 0$ case. In the presence of distortions we can see the

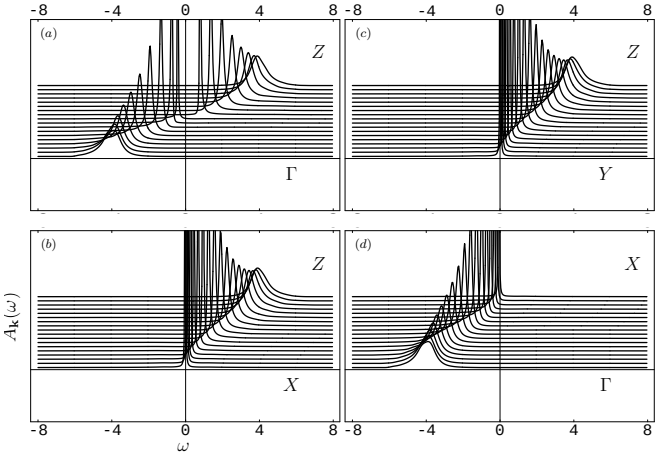

Fig. 7. Spectral function for the lines $\Gamma \to Z$, $Y \to Z$, $X \to Z$ and $\Gamma \to X$. The line in Fig. (a) is crossing the M point where there is no spectral peak as a result of the presence of a gap in the quasiparticle dispersion.

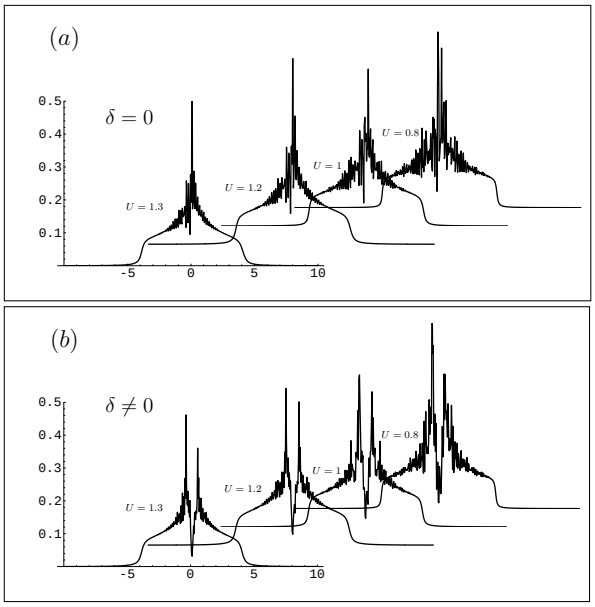

Fig. 8. a) Density of states $\rho(\omega)$ in the case with $\delta = 0$ for $U = 0.8$, $U = 1$, $U = 1.2$ and $U = 1.3$. The interaction gives a transfer of spectral weight from low to high energies. b) Density of states $\rho(\omega)$ in the presence of elastic distortions for $U = 0.8$, $U = 1$, $U = 1.2$ and $U = 1.3$.

absence of a spectral peak for some points around $\omega = 0$ which shows the existence of a gap at these points in the renormalized dispersion. There are no possible low-energy excitations with $\Xi \approx 0$ at these points of the BZ.

The density of states was calculated for fixed values of the chemical potential μ and the Coulomb interaction U.

$$g(\omega) = \frac{1}{L} \sum_{\mathbf{k}} A_{\mathbf{k}}(\omega) \tag{24}$$

In Figure 8 the renormalized density of states is shown for both phases at $\rho = 0.995$ with $U = 0.8$, $U = 1$, $U = 1.2$ and $U = 1.3$. The interaction gives a transfer of spectral weight from low to high energies in both cases.

In the absence of distortions the weight of the logarithmic singularity which characterizes the free system is reduced. Similar characteristics of $g(\varepsilon)$ are obtained for the infinite-dimensional Hubbard model [21]. Large U values give rise to the typical two-peaks situation corresponding to the infinite U limit.

2.5 Fermi Surface in the presence of distortions

The solutions of $\omega - \xi_{\mathbf{k}} - \Re e\Sigma(\mathbf{k}, \omega) = 0$ determine the renormalized dispersion $\Xi_{\mathbf{k}}$, the points where $\Xi_{\mathbf{k}} = 0$ define the interacting FS. When we analyze the Hubbard Model without elastic distortions a point with $\Xi_{\mathbf{k}} < 0$ is inside of the Fermi Area and if $\Xi_{\mathbf{k}} > 0$ it is outside. In the present case we need to be careful with this interpretation; a point with $\Xi_{\mathbf{k}} < 0$ can be inside the Fermi Area or at

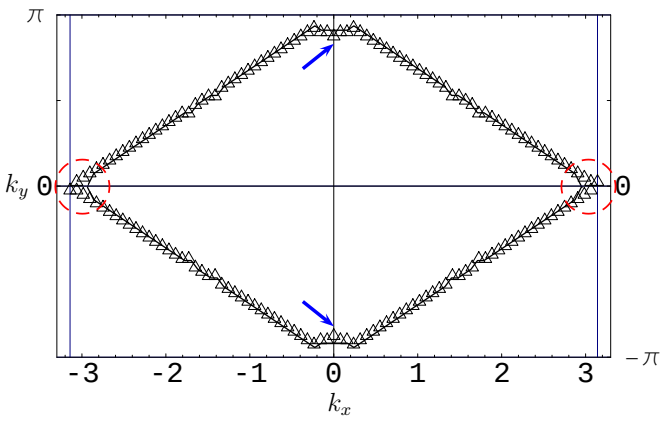

Fig. 9. Interacting Fermi Surface for $U = 0.8$, $\mu = -0.1$ and $\delta = 0.24$. The red circles mark the zones where the surface stretches in the k_x-direction and the blue arrows the zones where the surface is contracted in the y-direction.

the FS depending on whether the point coincides with the gap in the renormalized dispersion relation.

The interacting FS for $\delta = 0.24$ and $\mu = -0.1$ is shown in Figure 9. The symbols correspond to $U = 0.8$ and the solid line to $U = 0$. We can see that the effect of the interaction leads to an anisotropic surface resembling a nematic phase FS. The points in the interacting FS evolve so that the point on the k_x-axis comes closer to the X point and the point on the k_y-axis moves away from the Y point when the interaction is increased. We do not see any change in FS topology. This result is consistent with earlier works [12] and shows that interactions do not modify the FS topology within the perturbatively controlled weak coupling regime.

3 Discussion and Summary

The Hubbard model on the square lattice in the weak coupling regime in the presence of lattice distortions that follow Peierls-like patterns was investigated.

Using second order perturbation theory, several spectral properties are calculated and compared with the Hubbard model in the absence of lattice distortions. The stability of the distortions was analyzed as a function of U and λ finding that the Coulomb interaction suppresses the lattice distortions for values of U_c smaller than previous MF results and a schematic phase diagram is presented.

The results show that the Interacting Fermi Surface is anisotropic in the presence of distortions, even in the weak coupling regime. The Fermi Surface topology does not change in any of the two phases. This result is consistent and complementary with earlier results [12] where the stability of the FS topology in the absence of distortion has been analyzed previously by Metzner *et al* in the weak coupling regime . The results presented in this paper show a similar behavior in the presence of distortions.

ACKNOWLEDGMENTS

We would like to thank D.C. Cabra, G. L. Rossini and H.D. Rosales for helpful discussions. This work was partially supported by ECOS-Sud Argentina-France colaboration (Grant No A04E03), PICS CNRS-Conicet (Grant No. 18294), PICT ANCYPT (Grant No 20350), and PIP CONICET (Grant No. 5037).

References

1. We take the lattice spacing $a = 1$.
2. Yucel Yildirim, Adriana Moreo, cond-mat/0503292 (2005)
3. W. Kohn, J. M. Luttinger, Physical Review **118**, 41 (1960).
4. J. M. Luttinger, J. C. Ward, Physical Review **118**, 1417 (1960).
5. J. M. Luttinger, Physical Review **119**, 1153 (1960).
6. C.A. Lamas, D.C. Cabra, N. Grandi, arXiv:0804.4422 (2008).
7. The Theory of Superconductivity in the High-Tc Cuprates . P. W. Anderson (1997) Princeton University Press
8. B. Valenzuela, M. A. H. Vozmediano; Phys. Rev. B **63**, 153103 (2001).
9. Hidekazu Nojiri, cond-mat/9812358 (1998).
10. K. Shonhammer and O. Gunnarsson, Phys. Rev. B **37**, 3128 (1988).
11. W. Metzner, D. Rohe and S. Andergassen Phys. Rev. Lett. **91** 066402 (2003).
12. C. J. Halboth, W. Metzner, Z. Phyz B **102** 501 (1997).
13. C. J. Halboth, W. Metzner, Phys. Rev. Lett. **85**, 5162 (2000).
14. H. Fehske, D. Ihle, J. Loos, U. Trapper, H. Biittner, z. Phys. B **94**, 91 (1994).
15. J. Riera and A. Moreo, Phys. Rev. B **37** 9546 (1987).
16. The pattern (a) has two possible accomplishments, with $\delta^x = 0$ or $\delta^y = 0$.
17. S. Tang and J. E. Hirsch, Phys. Rev. B **73** 014518 (2006).
18. Qingshan Yuan, Thilo Kopp, Phys. Rev. B **65** 085102 (2002).
19. V. Zlatic, K. D. Schotte, G. Schliecker; Phys. Rev B **52**, 3639 (1995).
20. G. D. Mahan, Many-Particle Physics, Plenum Press,New York (1981).
21. N. Bulut, D. J. Scalpino, and S.R White; Phys. Rev. Lett. **72**, 705 (1994).